Heliyon 7 (2021) e07542

Contents lists available at ScienceDirect

Heliyon

journal homepage: www.cell.com/heliyon

Research article

A simple platform for the electro-catalytic detection of the dimetridazole using an electrochemical sensor fabricated by electro-deposition of Ag on carbon graphite: application: orange juice, tomato juice and tap water

Jallal Zoubir *, Idriss Bakas, Ali Assabbane

Laboratory of Catalysis and Environment, Faculty of Science, Ibn Zohr University, BP 8106 Cité Dakhla, Agadir, Morocco

ARTICLE INFO

Keywords:
Silver microparticles
Electro-deposition
Anti-protozoal
Dimetridazole
µAg@CPE

ABSTRACT

The objective of this paper is to evaluate and optimize the experimental parameters of the electro-deposition of silver atom nuclei on a graphite carbon paste to elaborate an electrochemical sensor. The electro-deposition process was performed using the cyclic voltammetry. The electrochemical studies show that the deposited silver micro-particle array offers an excellent electro-catalytic activity towards the NO_2 attractor group of the dimetridazole side chain. SEM morphological analysis of the silver deposits indicates the presence of a large number of Ag micro-particles on the graphite carbon with good nucleation. The size of the Ag micro-particles is of the order of 19,7621 µm and their distribution is normal over the entire range of the pulp. DRX analysis of the deposit also indicates that the microcrystalline structure of the silver microcrystals in the deposit is face-centered cubic. The electrochemical behavior of dimetridazole is totally irreversible, the transfer process is controlled by diffusion phenomena on the surface of the electrode covered by a silver deposit realized µAg@CPE. The analytical performance of the constructed electrode shows a good selectivity. Calibration curves for the detection of dimetridazole have been drawn in the concentration range of $3{,}5 \times 10^{-4}$ mol/L to 10^{-6} mol/L using cyclic voltammetry method, with a detection and quantification limits of 6.565×10^{-7} mol/L and 2.216×10^{-6} mol/L respectively. The applicability of the constructed electrode has been tested in real samples including orange juice, tomato juice, tap water. The results obtained show a recovery rate above 94%, which is very satisfactory.

1. Introduction

The active ingredient dimetridazole (DMT) [1,2-dimethyl-5-nitroimidazole] is an anti-protazaire and antibacterial of the imidazole class that has been used for more than 40 years [1]. Today, dimetridazole plays a very important role in veterinary medicine for the treatment of infections related to anaerobic and protozoan bacteria in animals [2] and is also one of the drugs used in the agricultural sector to promote animal growth. Consumption of dimetridazole in uncontrolled amounts may result in residues of dimetridazole metabolites in food products, with adverse effects on human health [3, 4, 5]. Because of the essential role of dimetridazole as an active ingredient in human health, its determination and detection in real samples and drug formulations are very important. In this context, we have developed an electrochemical sensor with a low content of silver nuclei deposited on carbon graphite, capable of detecting low concentrations of dimetridazole.

Various methods have been reported for the determination of the active principe dimetridazole in literature such as liquid chromatography [6], high-performance liquid chromatography-mass spectrometry [7, 8] gas chromatography [9, 10] adsorptive stripping voltammetry [11] These methods, although very cost-effective and efficient, are not available in many laboratories and are expensive to perform many analyses. Our research group has focused on the use of electrochemical techniques to detect dimetridazole using a carbon paste electrode modified with silver micro-particles. The paste modification process was carried out by electro-deposition techniques of thin layers of silver atomic nucleus arrays on carbon graphite. This modification of the electrode surface is carried out in order to increase the electro-catalytic effect of the working electrode and also to improve their analytical performance, that is to say to increase the sensitivity, to lower the detection limit, to widen the linearity range of the quantification of dimetridazole molecules.

In this work, we present a simple platform for the determination of the anti-protazaire dimetridazole in real samples. The µAg@CPE sensor

* Corresponding author.
E-mail address: zoubirjallal@yahoo.fr (J. Zoubir).

https://doi.org/10.1016/j.heliyon.2021.e07542
Received 15 March 2021; Received in revised form 6 May 2021; Accepted 7 July 2021

has been manufactured by an electro-deposition process of silver microparticles on carbon graphite. The reduction of Ag^+ ions on the surface of the working electrode leads to a nucleation of silver atoms of micrometric size allowing obtaining a higher sensitivity towards dimetridazole molecules, a very low ohmic loss compared to the unmodified carbon paste electrode. The influence of the different experimental parameters on the electrochemical deposition of silver was studied; the electro-catalytic performance and the electron transfer properties on the surface of the modified μAg@CPE electrode were examined by cyclic voltammetry and impedance spectroscopy. The influences of the main interferents on the response of the proposed constructed electrode were evaluated by cyclic voltammetry, the electrochemical platform that offers advantages such as greater simplicity, low cost and a very low detection limit for dimetridazole. Finally, the sensor suggests to demonstrate a better catalytic property during the dimetridazole reduction reaction in real samples such as orange juice, tomato juice and tap water with a low detection limit.

2. Experimental

2.1. Apparatus

The electro-catalytic silver metal deposition process was carried out using an Origa Master 5 potentiostat connected to an electrochemical cell. The electrochemical cell is composed of a solution of silver nitrate ($Ag^+ + NO_3^-$) and three electrodes such as a carbon graphite paste electrode which serves as a working electrode on which the electrodeposition is carried out. A reference electrode (RE) Ag/AgCl saturated by 0.3M the KCl, and a platinum wire as a counter electrode to supply the current (AE). All dates and experimental results have been processed using a personal computer which is connected to the Origa Master 5 potentiostat. Electrochemical impedance spectroscopy and cyclic voltammetry measurements were also performed using the same Origa Master 5 potentiostat. X-ray diffraction of the PERT-PRO (BRUKER-AXS) type with Cu_K radiation $\lambda_{cu} = 1.5406$ Å installed at the research unit of Ibn Zohr University of Agadir in Morocco was used to identify the nature of the different chemical compositions in the electrochemical silver deposition performed. The JEOL type SEM installed at the research unit of Ibn Zohr University of Agadir Morocco was used to visualize the image of the distribution of silver microparticles on the carbon graphites produced. The different measurements of pH values were made from pH meters of quality.

2.2. Reagents

Among the essential products we used in this work, the active principle dimetridazole, silver nitrate and carbon graphite (a very fine powder) were purchased from Sigma Aldrich. Other chemical reagents such as KH_2PO_4 and KH_2PO_4 $[Fe(CN)_6]^{3-/4-}$ were purchased from Fluka and were of standard analytical quality. PBS phosphate buffers (0.1 M) were prepared from KH_2PO_4 the 0.1 M and $K_2HPO_4$the 0.1 M as supported electrolytes. The pH of the phosphate buffers 0.1 M was adjusted by concentrated HCl or NaOH solutions.

2.3. Analytical procedure

We prepared the orange juice recipe, the oranges were purchased from a local supermarket. Two selected organs were carefully rinsed and cleaned to remove all traces of dust and pesticides. Half of the organ was removed and squeezed, using an electric centrifuge to extract all the juice, then filtered through a 20μm micropro filter paper several times. Take three vials of volume 200ml containing a volume of 180ml of phosphate buffer solution of pH = 7. Then pour into each vial a volume of 20ml of orange juice obtained. The three prepared orange juice sample vials. They were spiked with a precise amount of antiprotozoal dimetridazole to have final concentrations of 10^{-5} mol/L, 5 10^{-6} mol/L and 10^{-6} mol/L in each vial and left under stirring for 30min. Then the prepared samples were analyzed in the same way using the constructed electrode. The voltammograms were recorded under optimal conditions, the recovery rate was calculated from the calibration curves with the obtained regression equations.

For the red tomato juice recipe, we followed the following steps: Step 1: Two red tomatoes were thoroughly cleaned with distilled water to remove all traces of pesticides. Step 2: We cut the tomatoes into small pieces and put them in a blender to crush them. The juice obtained was filtered several times to remove all small seeds, taking three vials of volume 200ml containing a volume of 180ml of phosphate buffer solution of pH = 7. Then pour into each vial a volume of 20ml of the obtained red tomato juice. The three sample vials of red tomato juice prepared. They were spiked with a precise amount of antiprotozoal dimetridazole to have final concentrations of 5 10^{-6} mol/L, 2 10^{-6} mol/L and 10^{-6} mol/L in each vial and left under stirring for 30min. Then the prepared samples were analyzed in the same way using the constructed electrode. The voltammograms were registered under optimal conditions, the recovery rate was calculated from the calibration curves with the obtained regression equations.

Samples of tap water are used without any pretreatment.

2.4. Electrochemical measurement

All electrochemical experiments were performed using the electrode which was constructed by electro-deposition of silver under optimal conditions. The electrochemical deposition of silver on carbon graphite was carried out using the cyclic voltameter method. Cyclic voltammograms of dimetridazole detections were recorded in the potential range from 00mv to -1200mv. The Nyquistes carried out were carried out in the frequency range going from 10KHz to 10Hz with an amplitude of 10 mV, the recovery rate was calculated from the calibration curve with regression of the equation the latter is traced by the cyclic voltammetry method.

All electrochemical experiments were performed using the electrode constructed by silver electro-deposition under optimal conditions mentioned in The Table 1. The electrochemical deposition of silver on carbon graphite was performed using the cyclic voltammetry method. The cyclic voltammograms of the dimetridazole detection and interferences effects were realized in conditions following the range of potential used between 00 mV to -1200 mV, scan speed v = 20mv/s, pH = 7.

3. Results and discussion

3.1. Electrodeposition of Ag on carbon graphite

Figure 1A Shows the cyclic voltammograms obtained from the electro-deposition of silver micro-particles on the surface of carbon graphite paste that were performed by the cyclic voltammetry in the potential range of 800mv to 00mv using an electrolytic bath of phosphate buffers containing silver ions. The results obtained show that the selected potential range is very favorable for the reduction of silver ions. Moreover, it is observed that the ion reduction peak is localized in the 0.4V vs AgCl positions, the electrochemical behavior of silver is totally reversible

Table 1. Groups together the various parameters optimized during the electrodeposition process.

Influence of parameter variables	Optimizes
The supporting electrolyte	PBS
pH	2
The sweep rate of the potential	5mv/s
The concentration of silver ions Ag^+	8 10^{-3} mol/L
The number of scan cycles	2

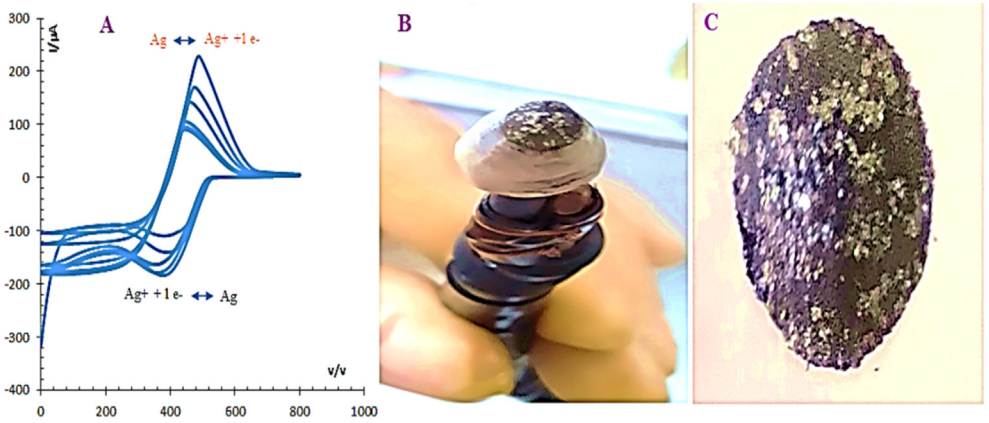

Figure 1. CVs of silver electro-deposition on a carbon graphite paste (A). The real image of the working electrode with electrochemical deposition of Ag (B). The image of the carbon paste constructed with silver deposition (C).

as indicated by the cyclic voltammograms obtained. The current density of the redox peaks decreases progressively as the cyclic number increases which means that the nucleation of the silver atoms is blocked thanks to the saturation of the electrode surface which will push the silver ions towards the solution and block the transfer of electrons to the surface. This blocking has prevented the reduction of Ag^{+} ions has become difficult on the electrode surface, therefore, it has limited the reduction reaction of Ag^{+} ions.

Finally, a decrease in the consumption of Ag^{+} ions which leads to a decrease in current density. In the same figure, we can also see the real image of the working electrode (Figure 1B) with the paste that is partially covered with an electrochemical silver deposit. The last image represents the real image of the silver layer deposited on the carbon graphite paste (Figure 1C). These results suggest that the silver nucleation processes were well executed. The selection of the working electrode surface geometry allows the multiplication of active sites and improves the sensitivity of our constructed electrodes.

In order to obtain a good electro-catalytic performances for our sensor, we have started to optimize all experimental parameters of the electro-deposition process, including pH of the electrolyte solution, scanning speed, number of cycles, and silver concentration in the electrolyte solution. This approach allows us to improve the electro-catalytic performances of the silver layer developed for the detection of dimetridazole. On the other hand, the developed electrochemical sensor must support a high number of electrochemical measurements performed, also supports the number of regeneration steps of the agent layer deposited on the carbon paste to maintain the electro-catalytic properties when used in semi-continuous or continuous mode.

3.2. Optimization of silver electro-deposition parameters

The first studied parameter is the effect of the support electrolyte pH on the silver electro-deposition, the range of pH extends from 1 to 5. The best results obtained (in terms of current intensity and displacement of the dimetridazole cathodic peak) were brought to the phosphate buffer electrolyte solution with a pH = 2 (Figure 2A). This means that the best nucleation of the silver micro-particles on carbon was obtained at this pH = 2 value, resulting in a strong electro-catalytic activity towards the reduction of dimetridazole molecules. Therefore, phosphate buffer at pH = 2 is the ideal case for the electro-deposition of silver on carbon graphite.

Figure 2B Illustrates the influence of the scanning speed of Ag electro-deposition on the intensity of the electro-catalytic current of the dimetridazole reduction. According to the results obtained, the best sensitivities of the elaborated electrode were carried with a potential scanning rate v = 5mv/s to carry out the silver electro-deposition. On the other hand, the increase of the electro-deposition speed decreases the sensitivity of our elaborated electrode due to the fact that the nucleation processes of silver micro-particles during the electro-deposition are not well detected and observed by cyclic voltammetry.

The effect of the silver ions concentration in the electrolytic bath was investigated in the tested concentration range of 1.0×10^{-3} mol/L to 10^{-2} mol/L [$AgNO_3$] at pH = 2. The results (Figure 2C), show that the best electro-catalytic performances in terms of current moves to positive values when the concentration of Ag ions in the electrolyte bath is $8\ 10^{-3}$ mol/L. These results suggests that the mass of the layer of micro-particles deposited on the surface of the electrode is highly conductive and that the

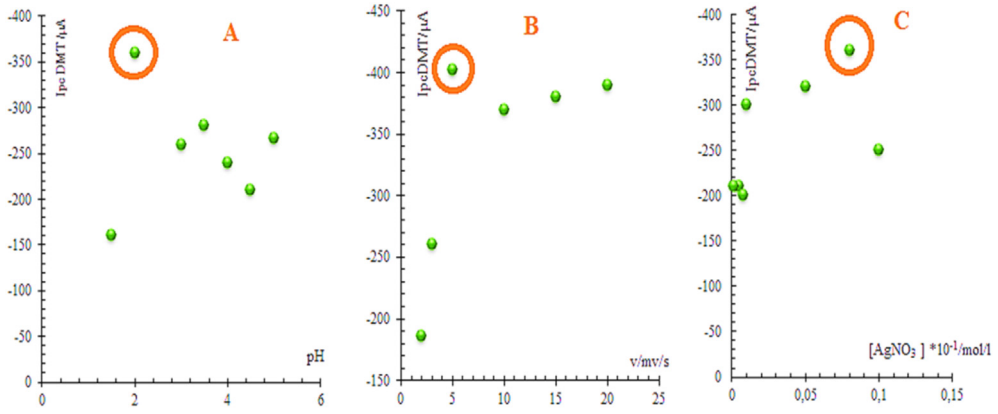

Figure 2. Curves A; B and C show the influence of the experimental variables of Ag electro-deposition on the cyclic voltammetry response of 10^{-3} mol/L dimetridazole in PBS buffer pH = 7.

coverage of the surface is partial. Therefore, the optimal concentration for silver electro-deposition is set around 8 10^{-3} mol/L of the [$AgNO_3$].

The performances of the constructed electrode depend also on the number of scanning cycles. According to the results illustrated in Figure 3A, the number of scanning cycles allowing a good electro-catalytic detection of dimetridazole were about n = 2, reflecting the fact that the electrode surface is not completely covered by a thin film of silver micro particles. But the increase in the number of scanning cycles causes a layer of silver micro particles with a very strong mass which considerably decreases the sensitivity of the electrode surface as shown in the obtained cyclic voltammogram (Figure 3B).

3.3. Characterization of the prepared electrodes

3.3.1. Observation by scanning electron microscopy

Figure 4A shows the SEM image of the electrochemical deposition carried out on the carbon graphite paste. It can be seen that the surface of the paste is largely covered by silver microparticles of very similar size and dispersed over the entire surface of the paste. This result confirms that the nucleation of the silver microparticles is immobilized on most of the surface of the carbon graphite paste and that the Ag atoms produced by the reduction reaction of Ag^+ ions have been triggered in an Ag lattice providing a good electro-catalytic capacity on the surface of our elaborated electrode. And that the range of potentials applied during the Ag electro-deposition is very favorable to form a silver layer on the carbon graphite sheets. The results obtained are very coherent with the results reported by A.M.Fekry et al [12, 13, 14].

The DEX analysis (Figure 4B) illustrates the presence of peaks corresponding to silver at the position of 2 Kev; 2.3 Kev; 2.5Kev and a carbon peak. The results suggest the presence of silver atomic nuclei with a remarkable amount. The DEX analyses obtained were very close to that published by A.M. Fekry et All [15, 16].

3.3.2. Analysis of μAg@CPE by X-ray diffraction and histogram of the diameter distribution of Ag

The nucleation of silver atoms on the carbon paste under optimized conditions was confirmed by recording the X-ray diffraction spectrum. The spectrum obtained shows the presence of the five new peaks compared to the carbon spectrum of graphite alone Figure 5A.

Five peaks appear, located at the respective angles 2θ° = 37.95°; 44.33°; 64.5°; 77.35° and 81.8°. This means the formation of a new metallic phase based on silver. The folder (JCPDS, folder no. 4-0783) [17] allows these peaks to be attributed to the Ag phase. Which has a face-centered cubic structure. The calculated mesh parameter a= 4.081 ± 0.0027Å. These results clearly confirm that the silver electro-deposition process on the carbon paste was well performed under the optimized experimental conditions.

The Figure 5B, illustrate histograms of the diameter distribution of Ag microparticles. The size and distribution of silver microparticles on the surface of the electrode paste was evaluated from the SEM image obtained in Figure 4A. The mean size of the large number of silver microparticles was calculated using a computer system at is estimated to be 19.7689μm and (SD = 2.712) with a normal distribution. This result shows very precisely the fundamental role of the small size of silver atoms in electro-catalysis for the reduction of the dimetridazole attractor group.

Therefore, the creation of a micrometric array of silver nuclei on the surface of the working electrode, with a homogeneous distribution, reflects a large active surface area that ensures a greater chance of contact with the electro-active dimetridazole molecules, as well as a strong electro-catalytic effect to transform the NO_2-attracting groups of the antiprotozoal dimetridazole molecules into NHOH groups.

3.4. Electrochemical behaviors of DMT on the μAg@CPE

3.4.1. Electro-catalytic reduction of DMT on the μAg@CPE and CPE Nu

The electrochemical behavior of dimetridazole was evaluated on the two constructed μAg@CPE electrode and the unmodified CPE electrode. The cyclic voltammograms (Figure 6) obtained using these electrodes, show that a small peak of cathodic reduction of dimetridazole was observed at a potential equal to -710mv by the unmodified CPE electrode relative to Ag/AgCl, which can be explain by the very slow kinetics of electron transfer at the surface of the CPE. On the other hand, a very wide and well-defined cathodic dimetridazole reduction peak was observed on the constructed electrode at a potential equal to -560 mv with respect to Ag/AgCl, which means that the number of antiprotozoal dimetridazole molecules trapped on the surface of the constructed electrode is very large with a very short time. With a potential difference equal to -150 mv with respect to the carbon electrode alone, which shows that the transfer of electrons to the surface of the modified electrode is very fast. Moreover, by noticing that in the opposite direction of the anodic scanning in the volammograms at both electrodes, no oxidation peak is observed. This indicates that the behavior of the antiprotozoal dimetridazole is absolutely irreversible.

Therefore, the shift of the peak to positive potentials and the increase of the dimetridazole reduction peak Current at the surface of the proposed constructed electrode are due to the presence of a network of micrometer-sized silver atomic nuclei that increase the electro-catalytic effect of the dimetridazole reduction reaction.

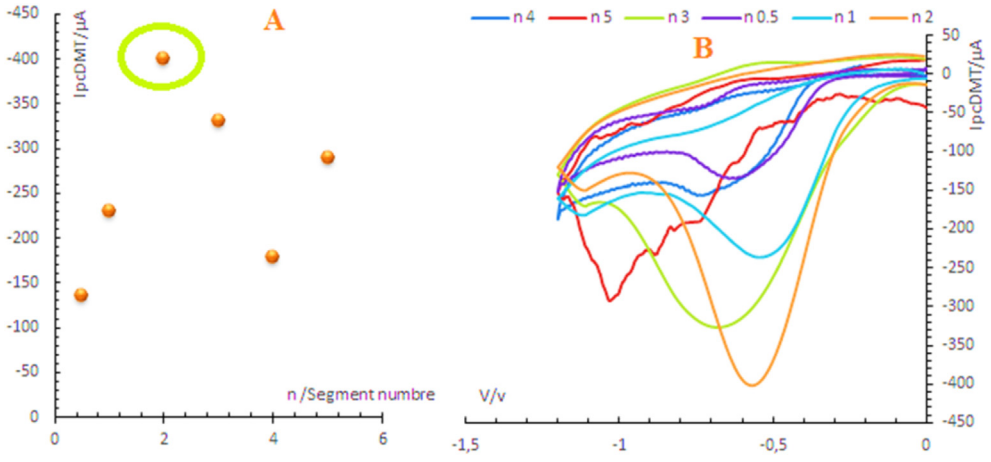

Figure 3. CVs of DMT detection (10^{-3} mol/L) using the constructed electrode at different numbers of cycles ranging from 0.5; 1; 2; 3; 4; 5 (B). Curve (A) represents the variation in the intensity of the electro-catalytic DMT current as a function of the number of cycles applied to the silver electrodeposition process.

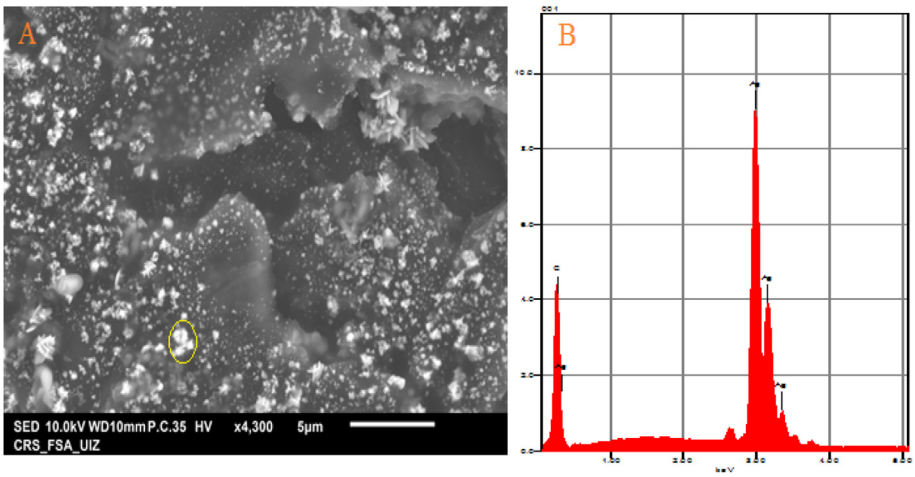

Figure 4. SEM image of µAg@CPE (A), EDX spectra of Ag@CPE (B).

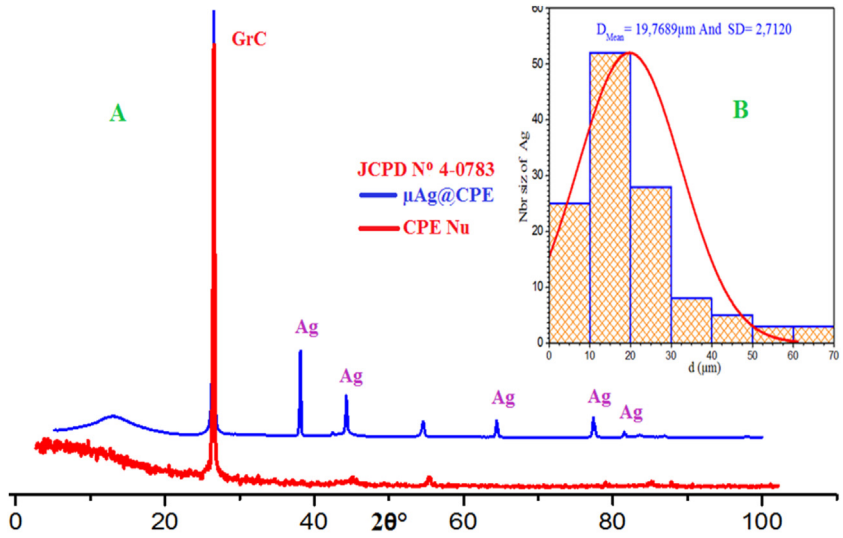

Figure 5. DRX of µAg@CPE and CPE (A). Histogram of the Ag diameter distribution on graphite carbon (B).

3.4.2. Comparison between fabricated µAg@CPE and CPE Nu using cyclic voltammetry

The electrochemical behavior of $[Fe(CN)_6]^{-3/4-}$was evaluated on the unmodified CPE and µAg@CPE electrode in the presence of 1 mM $[Fe(CN)_6]^{-3/4-}$and 0.5 M of KCl (Figure 7A). The comparison between the obtained cyclic voltammograms shows a very strong improvement of the current intensity of the oxidation and reduction peaks of the $[Fe(CN)_6]^{-3/4-}$redox probe using the electrode constructed by silver electroplating µAg@CPE almost 4 times compared to the unmodified CPE electrode. This increase reflects the role of the arrays of electrochemically deposited Ag microparticles on the highly conductive carbon graphite sheets that promote the reduction reaction of ferrocene ions at the surface level of the µAg@CPE electrode. There is also a remarkable decrease in the potential difference ΔE_{pac} between the two anodic and cathodic $[Fe(CN)_6]^{-3/4-}$peaks, ΔE_{pac}(CPE) = 300mv and ΔE_{pac}(µAg@CPE) = 60mv. This reflects that the electron transfer kinetics of the electrolyte/electrode interface using µAg@CPE is very fast compared to the unmodified CPE electrode.

3.4.3. Comparison between µAg@CPE and CPE by using impedance spectroscopy

In order to fully understand the interface between the fabricated sensor and the electrolyte using electrochemical impedance spectroscopy. The electro catalytic realization of µAg@CPE and CPE was performed by EIS using 5Mm of $[Fe(CN)_6]^{-3/4-}$ with 0.1M KCl as

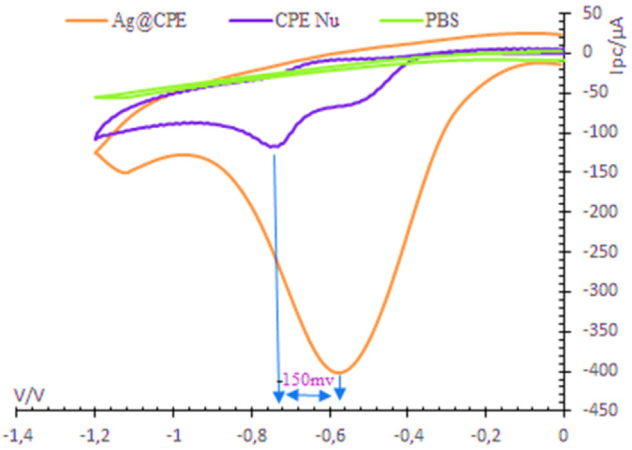

Figure 6. CVs of dimetridazole using µAg@CPE and unmodified CPE electrodes, in PBS (pH = 7) with a sweep rate of 20mv/s.

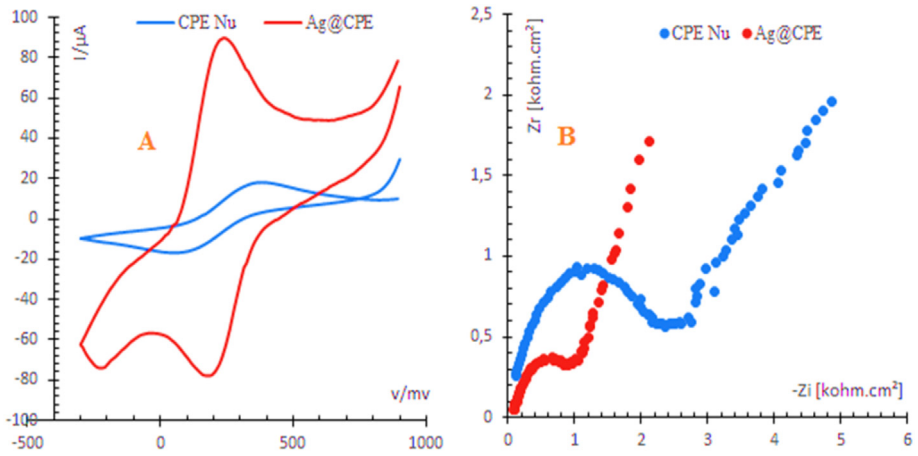

Figure 7. CVs of the unmodified CPE and µAg@CPE built at 50 mvs^{-1} (A). Nyquist diagram of the unmodified CPE and µAg@CPE (B) in 1mM $[Fe(CN)_6]^{3-/4-}$ containing 0.1 M KCl at 10 KHz to 100 Hz.

electrolyte support in a frequency ranging from 10KHz to 100HZ with an amplitude of 10mv and an applied potential of -450mv (Figure 7B).

The Nyquist results obtained show that the charge transfer resistance at the surface of the unmodified CPE electrode was equal to $R_{ct} = 2.6$ kΩ/cm^2 which reflects that the electrostatic attraction between the negatively charged ions of the redox probe $[Fe(CN)_6]^{-3/4-}$and the surface of the CPE electrode is very blocking. We also observe a strong decrease in the resistance to charge transfer at the µAg@CPE electrode surface, with R_{ct} (µAg@CPE) = 1.2 kΩ/cm^2. This means that the electrostatic attraction between the surface of the proposed modified electrode and the $[Fe(CN)_6]^{-3/4-}$couples is very strong. Indicating that the nucleation processes followed to build the film of silver microparticles deposited on

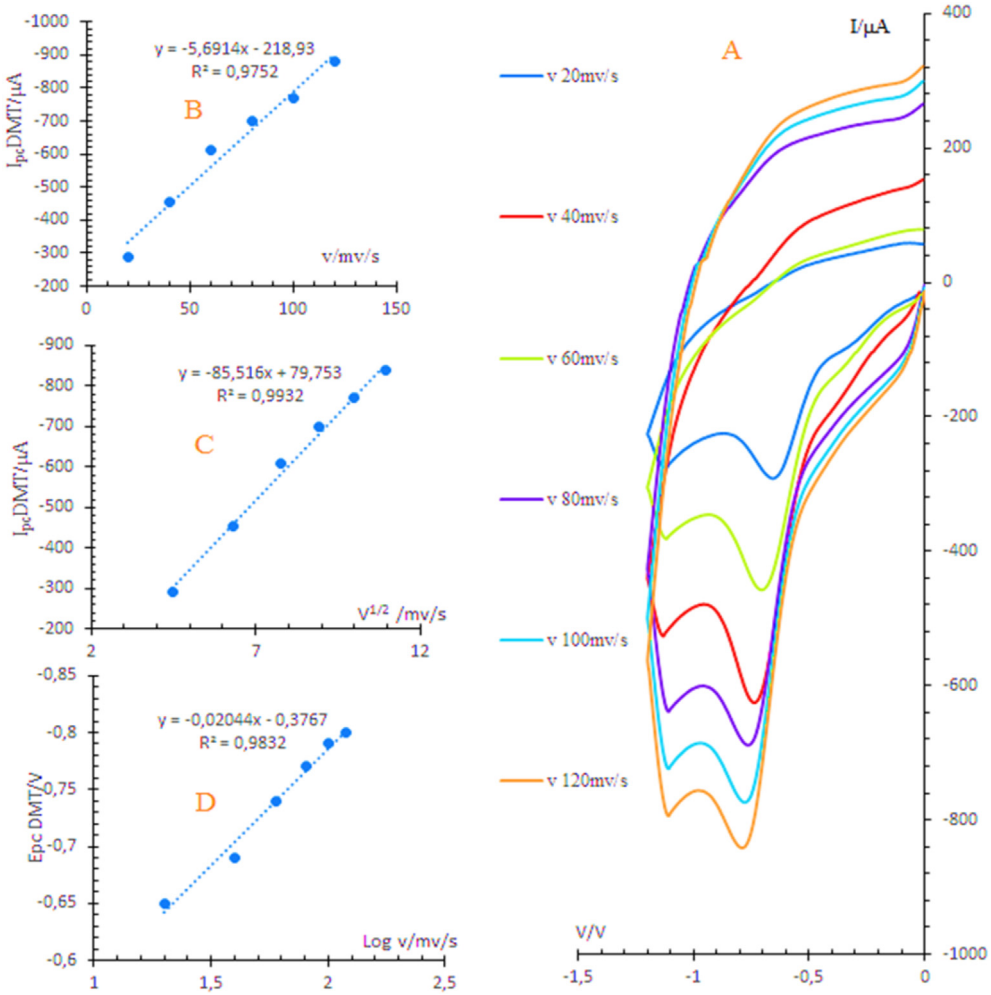

Figure 8. CVs responses of 1 mM the DMT on the µAg@/CPE with different scan rates (20-120 mV/s) at pH = 7 (A). The I_{DMT} calibration curve as a function of v(mv/s). (B) and plot of the I_{DMT} as a function of $v^{1/2}/(mv/s)^{1/2}$ (C) and the E_{pc} variation (DMT) as a function of Log v. mv/s (D).

Table 2. The influence of coexisting substances on the detection of 1.0×10^{-4} mol/L of dimetridazole (n = 3).

Coexisting substance	Concentration de Coexisting substance (mmol L^{-1})	Change of peak current (%)	Coexisting substance	Concentration de Coexisting substance (mmol L^{-1})	Change of peak current (%)
Cl	1	-0,66	CO_3^{2}	1	0,54
Fe^{3+}	1	-1, 50	K^{+}	1	-1,4
NO_3	1	-2,22	Ca^{2+}	1	-1,3
SO_4^{2}	1	-3	I	1	-0,86
Ni^{2+}	1	-2,3	Cu^{2+}	1	-0,7
Al^{3+}	1	-0,57	Zn^{2+}	1	-2,40
Na^{+}	1	0,70	Mg^{2+}	1	-1,35

the carbon play an important role in the electron transfer between the surface of the proposed modified electrode and the supporting electrolyte. A frequency-based straight line corresponding to diffusion is observed.

As a result, the deposited arrays of silver microparticles create highly conductive bridges that greatly increase the electrical conductivity of our electrode.

3.5. Effect of scan rate

As illustrated by the cyclic voltammograms performed using the silver electrode built-up under the previously reported optimized conditions (Figure 8), the potential scanning rate has an effect on the electro catalytic current intensity and the peak potential of the dimetridazole reduction at the surface of the built-up electrode. It can be seen that the peak potential E_{pc}(DMT) has been shifted to more negative values with increasing values of the scanning rate.

Figure 8A. Shows that the peak cathode current of the dimetridazole reduction increases linearly with the sweep rate of the potential in the range of 20 to 120mv/s with a regression equation I_{pc}(DMT) = -5.6914v -218.93(R^2 = 0.9752). The same observation was made when the variation of the maximum DMT current intensity as a function of the square root of the potential sweep rate plotted in the Figure 7C. With the regression equations I_{pc}(DMT) = -85.516$v^{1/2}$-79.753 and the correlation coefficients (R^2 = 0.9932). The linearity between the electro catalytic reduction current density of dimetridazole and the scanning speed confirms the presence of strong diffusion of a large number of molecules of the antiprotozoal dimetridazole on the surface of the modified working electrode. This means that the reduction reaction of the NO_2 attractor group of the dimetridazole molecules is controlled by diffusion regime processes. This phenomenon is very similar to that obtained by Murugan Keerthi et al [18]. This conclusion represents an ideal case for quantitative determination of the antiparasitic drug dimetridazole in real samples.

Figure 8D clearly shows that the peak reduction potential of dimetridazole varies linearly as a function of the logarithm of the scan speed Log(v) with a regression equation E_{pc}(DMT) = 0.3767–0.02044Log(v) with (R^2 = 0.9832). However, the electrochemical behavior of dimetridazole is totally irreversible as demonstrated by the voltammograms obtained, according to Laviron theoretical equation (Eq. (1)) defined by the following equation [19].

$$\mathrm{Epc(DMT)} = \mathrm{E_0} - \frac{RT}{\alpha nF}\left[0.780 + \log\left(\frac{\sqrt{D}}{k}\right) + \log\left(\frac{nF\alpha v}{RT}\right)^{1/2}\right] \quad (1)$$

$$\mathrm{Epc(DMT)} = \mathrm{E_0} + \frac{RT}{(1-\alpha)\,nF}\log(v) \quad (2)$$

R is the perfect gas constant (8.31J.K^{-1} mol^{-1}),T is the ambient temperature (298k), F is the shielding constant (96500C),α is the electron transfer coefficient,n is the number of electrons captured by the dimetridazole molecules to be reduced on the electro-catalytic surface of our sensors constructed.

In fact, for a totally irreversible system, α is estimated to have a value of 0.5, so, according to the slope obtained between Epc - Log(v) and the slope RT/((1 - α) nF) of Laviron theoretical equation (Eq. (2)), αn is estimated to have a value of 1.86. Therefore, the number of electrons (n) transferred to the surface of the electrode modified for electro-reduction of the dimetridazole NO_2 electro-active group is equal to 3.89 (approximately equal to 4).

3.6. Effect of the pH

The effect of the pH of the phosphate buffer solution ranging from 3.6 to 9 was studied using the electrode constructed by silver electrodeposition Figure 9A. Illustrates the cyclic voltammograms obtained for dimetridazole (10^{-3} mol/L) at different pH values with a scanning rate v = 20mv/s and an applied potential range of 00mv to -1200mv.

Figure 9A shows the linearity obtained between the variation in pH values and the peak reduction potential of dimetridazole. Regression equation obtained E_{pc}(DMT) = -0.056pH-0.2596 (R^2 = 0.9845) indicating that the slope obtained is almost very close to the value of the slope of the theoretical NERNST equation. This result reflects that the number of protons participating in the reduction reaction of dimetridazole molecules on the surface of the electrode constructed by electro-deposition of Ag on graphite carbon paste is equal to the number of electrons m/n = 1. This is numerically justified by the comparison between the numerical value of the slope (-0.056) obtained using equation and the numerical value of the slope of the theoretical equation NERNST (Eq. (3)) which are very close to each other.

$$\mathrm{Epc(DMT)} = \mathrm{E^{\circ}} - \left(\frac{2,303mRT}{nF}\right)\mathrm{pH} = \mathrm{E^{\circ}} - 0,059\frac{m}{n}\mathrm{pH} \quad (3)$$

m is the number of proton, n is the number of electrons.

Therefore, the electro-active –NO_2 groups in the side chain of dimetridazole are converted to NHOH when the reduction reaction is carried out on the surface of the constructed electrode. This result is very consistent with the work published by Murugan Keerthi and All [18].

The mechanism most likely to reduce dimetridazole on the silver micro particle arrays deposited on the carbon sheets of graphite was illustrated in Figure 10.

This mechanism that we have proposed is probably very similar to the one proposed by the work published by [20, 21, 22].

3.7. Interference

The effects of the principles interferences probably existing in the three selected samples such as: K^{+}, Ca^{2+}, I^{-}, Zn^{2+},Cl^{-},Fe^{2+}, NO^{3-}, SO_4^{2-}, Cu^{2+}, Mg^{2+},Ni^{2+},Al^{3+}, Na^{+}, CO_3^{2-}, on the response of the constructed electrode were examined under the optimal conditions described above. 200 ml of PBS were doped with an amount of dimetridazole to give a 10^{-4} mol/L. Then different amounts of interference were added. The solutions obtained were analyzed by cyclic voltammetry using the μAg@CPE sensor the results were summarized in Table 2. The peak current of the dimetridazole reduction does not interfere much compared

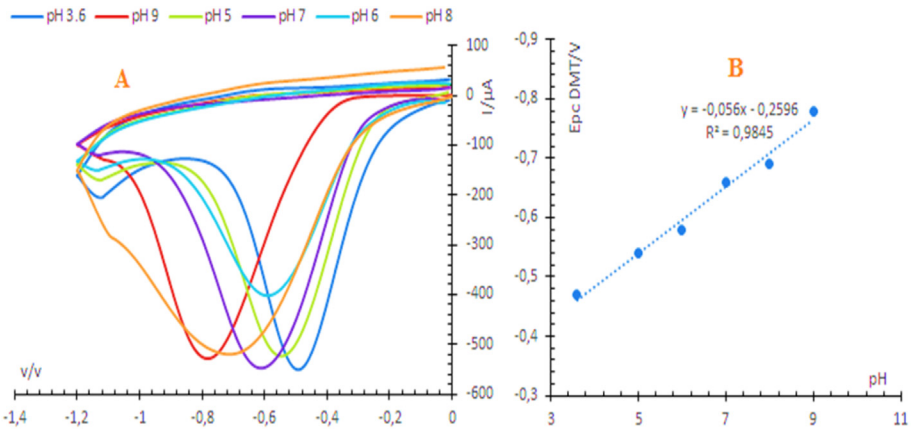

Figure 9. (A) CVs response of the constructed µAg@/CPE electrode in 1 mM of dimetridazole at different pH {pH: 3.60 to 9.00} at a scan rate of 20 mV/s. (B) The linear curve of pH versus E_{pc}(DMT).

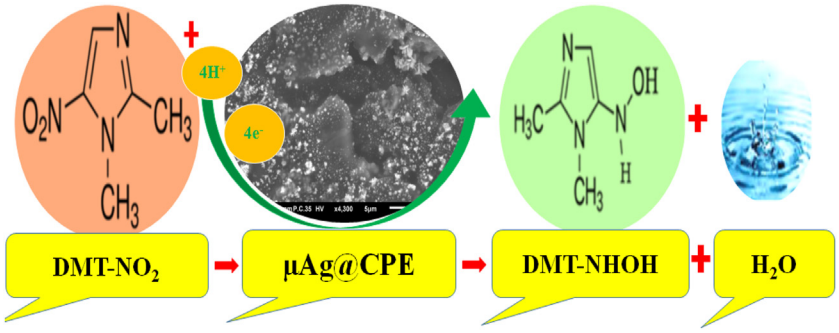

Figure 10. The dimetridazole reduction reaction mechanism at the electrode surface constructed µAg@CPE.

to the initial value of the current despite the presence of an excess of interfering substances such as 10 times K^+, Ca^{2+}, I^-,Cu^{2+}, Mg^{2+}, Zn^{2+},Cl^-, Cu^{2+}, Mg^{2+},Fe^{2+}, NO^{3-}, SO_4^{2-},Ni^{2+},Al^{3+}, Na^+, CO_3^{2-}. The relative standard deviation has been calculated to be no more than 5.4%, which means that the sensor is perfectly suited for dimetridazole analysis in complex matrices.

4. Determination of the antiprotozoal dimetridazole using µAg@CPE

The analytical utility of our µAg@CPE constructed electrode has been realized in the detection of the dimetridazole in real samples intended for human commsomation: tomato juice, orange juice and tap water.

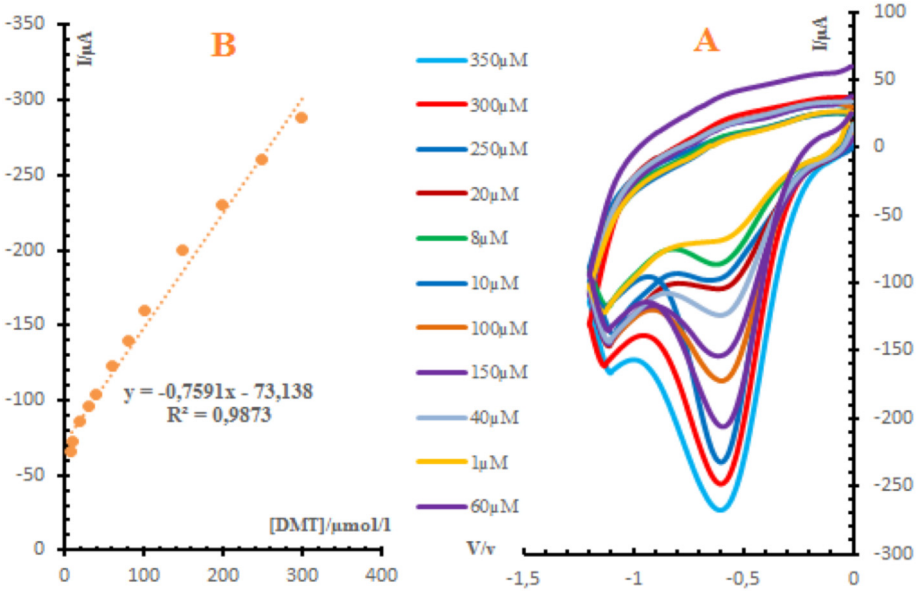

Figure 11. (A) Responses of CV to a decreasing concentration of DMT {350,300,250,150,100,60,40,20,10,8,1µM } on µAg@CPE in 0.1 mol L^{-1} PBS at pH = 7. (B) With the corresponding linear regression Ipc (DMT) as a function of the [DMT].

Table 3. Comparison of the performances of our μAg@CPE electrode to different techniques in the literature.

Electrod modifier	Method	L.range mol/l	LD (mol/l)	Ref
MIP-mimetic enzyme	DPV	0.5–1000 μmol/l	0.12 μmol/l	[23]
-	Gas	-	0.1–0.6 μmol/l	[24]
-	chromatography-electron capture negative ionization mass spectrometry	0–100 μmol/l	0.5 μmol/l	[25]
-	HPLC-UV Detection L.chromatography-Tandem mass spectrometry	–10 μmol/l	0.5 μmol/l	[26]
μAg@CPE	CVs	$3{,}510^{-4}$- 10^{-6} mol/l	0.6565 μmol/l	This work

Table 4. Recovery % of spiked dimetridazole from real samples.

Sample	Spiked(μM)	Found(μM)	Accuracy %	RSD%(n = 3)
Organ juice + DMT	10	9,76	97,6	1,22
	5	4,82	96,4	3,83
	1	0,976	97,6	1,34
Tomato juice + DMT	5	4,94	98,8	2,15
	2	1,97	98,5	3,33
	1	0,948	94,8	4,09
Tap water + DMT	5	4,91	98,1	2,32
	2	1,96	98	2,21
	1	0,971	97,1	2,43

Figure 11B shows the variation of the electro-catalytic current for the reduction of the dimetridazole on the active surface of the electrode manufactured by silver electro-deposition under the optimal conditions previously evaluated as a function of the dimetridazole concentration. As can be seen in the calibration curves, there is good linearity in the studied range of dimetridazole concentration from $3{,}5 \times 10^{-4}$ mol/L to 10^{-6} mol/L with the linear regression equation I_{pc}(DMT) = -0.7591x[DMT]-73.138 with ($R^2 = 9873$).

According to the formulas LD = 3Sd/p and LQ = 10 Sd/p with Sd the standard deviation of the current measured for the dimetridazole reduction for 8 voltammograms of phosphate buffer solution support the electrolyte at pH = 7 and p is the slope of the analytical curves obtained. The detection limit and quantification limit were then $6{,}565 \times 10^{-7}$mol/Land $2{,}216 \times 10^{-6}$ mol/L respectively. For the relative standard deviation, we evaluated and found 4.09% and 1.22% respectively, which is relatively very small. The μAg@CPE electrode has a wide detection linearity range and a low relative standard deviation (see Table 3).

The applicability of the proposed modified μAg@CPE electrode in real samples was evaluated by the standard addition method. Three totally different real samples were chosen: tomato juice, orange juice and tap water which were treated by the same way and then spiked with one mass of dimetridazole to reach concentrations of. 10 μmol/L; 5 μmol/L; 1 μmol/L of orange juice and 5 μmol/L; 2 μmol/L; 1 μmol/L of tomato juice and tap water respectively. Table 4 shows the recovery rate for each sample which exceeded 94%. The results obtained are very satisfactory and encouraging for the analysis of dimetridazole by the μAg@CPE sensor constructed by silver electro-deposition.

Table 4 demonstrate that the proposed sensor can be successfully adapted to detect traces of the antibiotic DMT in real samples such as orange juice, tomato juice and tap water.

5. Conclusion

The metallic silver microparticles deposited on the carbon paste by electro-deposition processes offer great potential for improving the sensitivity and selectivity of the electrode constructed for the determination of the antiprotozoal dimetridazole, due to their excellent electro-catalytic capacity of the surface decorated with atomic nuclei of Ag and their superior electrical conductivity. The structural study by DRX confirms the crystalline phase of face-centered cubic metallic silver, the SEM analysis shows that the nucleation processes of the silver atoms were well executed, immobilization and repoisoning of a large number of metallic silver microparticles on carbon graphite sheets. Allowing the construction of an electrochemical sensor with a wide range of linearity from 3.5×10^{-4} mol/L to 10^{-6} mol/L and a very low detection and quantification limit LD = 6.565×10^{-7} mol/L and LQ = 2.216×10^{-6} mol/L respectively. The applicability of the developed electrode was tested on real samples; the recovery rate found ranged from 94% to 97%. The results obtained reflect the effectiveness of using the proposed electrode to determine traces of the antiprotozoal dimetridazole in real samples such as organ juice, tomato juice and tap water.

Declarations

Author contribution statement

Jallal Zoubir: Conceived and designed the experiments; Performed the experiments; Analyzed and interpreted the data; Wrote the paper.

Idriss Bakas, Ali Assabbane: Analyzed and interpreted the data; Contributed reagents, materials, analysis tools or data; Wrote the paper.

Funding statement

This research did not receive any specific grant from funding agencies in the public, commercial, or not-for-profit sectors.

Data availability statement

No data was used for the research described in the article.

Declaration of interests statement

The authors declare no conflict of interest.

Additional information

No additional information is available for this paper.

References

[1] L. Connolly, C.S. Thompson, S.A. Haughey, I.M. Traynor, S. Tittlemeier, C.T. Elliott, The development of a multi-nitroimidazole residue analysis assay by optical biosensor via a proof of concept project to develop and assess a prototype test kit, Anal. Chim. Acta 598 (2007) 155–161.

[2] L. Jokipii, A.M. Jokipii, Comparative evaluation of the 2-methyl-5-nitroimidazole compounds dimetridazole, metronidazole, secnidazole, ornidazole, tinidazole, carnidazole, and panidazole against Bacteroides fragilis and other bacteria of the Bacteroides fragilis group, Antimicrob. Agents Chemother. 28 (1985) 561–564.

[3] Y. Lin, Y. Su, X. Liao, N. Yang, X. Yang, M.M.F. Choi, Determination of five nitroimidazole residues in artificial porcine muscle tissue samples by capillary electrophoresis, Talanta 88 (2012) 646–652.

[4] J.L. Ré, M.P. De Méo, M. Laget, H. Guiraud, M. Castegnaro, P. Vanelle, G. Duménil, Evaluation of the genotoxic activity of metronidazole and dimetridazole in human lymphocytes by the comet assay, Mutat. Res. Fund Mol. Mech. Mutagen 375 (1997) 147–155.

[5] M. De Méo, P. Vanelle, E. Bernadini, M. Laget, J. Maldonado, O. Jentzer, M.P. Crozet, G. Duménil, Evaluation of the mutagenic and genotoxic activities of 48 nitroimidazoles and related imidazole derivatives by the Ames test and the SOS Chromotest, Environ. Mol. Mutagen. 19 (1992) 167–181.

[6] M. Petrović, B. Škrbić, J. Živančev, L. Ferrando-Climent, D. Barcelo, Determination of 81 pharmaceutical drugs by high performance liquid chromatography coupled to mass spectrometry with hybrid triple quadrupole–linear ion trap in different types of water in Serbia, Sci. Total Environ. 468–469 (2014) 415–428.

[7] G. Stubbings, T. Bigwood, The development and validation of a multiclass liquid chromatography tandem mass spectrometry (LC–MS/MS) procedure for the determination of veterinary drug residues in animal tissue using a QuEChERS (QUick, Easy, CHeap, Effective, Rugged and Safe) approach, Anal. Chim. Acta 637 (2009) 68–78.

[8] A. Gentili, D. Perret, S. Marchese, Liquid chromatography-tandem mass spectrometry for performing confirmatory analysis of veterinary drugs in animal-food products, Trac. Trends Anal. Chem. 24 (2005) 704–733.

[9] C. Ho, D.W.M. Sin, K.M. Wong, H.P.O. Tang, Determination of dimetridazole and metronidazole in poultry and porcine tissues by gas chromatography–electron capture negative ionization mass spectrometry, Anal. Chim. Acta 530 (2005) 23–31.

[10] J.-H. Wang, Determination of three nitroimidazole residues in poultry meat by gas chromatography with nitrogen–phosphorus detection, J. Chromatogr. A 918 (2001) 435–438.

[11] M.R. Ali, M.S. Bacchu, M. Daizy, C. Tarafder, M.S. Hossain, M.M. Rahman, M.Z.H. Khan, A highly sensitive poly-arginine based MIP as an electrochemical sensor for selective detection of dimetridazole, Anal. Chim. Acta 1121 (2020) 11–16.

[12] H.K.A. Elhakim, S.M. Azab, A.M. Fekry, A novel simple biosensor containing silver nanoparticles/propolis (bee glue) for microRNA let-7a determination, Mater. Sci. Eng. C 92 (2018) 489–495.

[13] A.M. Fekry, A new simple electrochemical Moxifloxacin Hydrochloride sensor built on carbon paste modified with silver nanoparticles, Biosens. Bioelectron. 87 (2017) 1065–1070.

[14] M.A. Ameer, A.M. Fekry, S.M. Azab, M. Shehata, Synthesis of a simply modified electrochemical nicotine sensor based on silver nanoparticles, Can. J. Chem. 96 (2018) 821–827.

[15] A. Fekry, M. Sayed, Electrochemical corrosion behavior of nano-coated Ti-6Al-4V alloy by a novel chitosan nanoparticles/silver nanoparticles in artificial saliva solution, Egypt, J. Chem. (2018), 0–0.

[16] A.M. Fekry, S.A. Abdel-Gawad, R.H. Tammam, M.A. Zayed, An electrochemical sensor for creatinine based on carbon nanotubes/folic acid/silver nanoparticles modified electrode, Measurement 163 (2020) 107958.

[17] B. Habibi, M. Jahanbakhshi, A novel nonenzymatic hydrogen peroxide sensor based on the synthesized mesoporous carbon and silver nanoparticles nanohybrid, Sensor. Actuator. B Chem. 203 (2014) 919–925.

[18] M. Keerthi, M. Akilarasan, S.-M. Chen, S. Kogularasu, M. Govindasamy, V. Mani, M.A. Ali, F.M.A. Al-Hemaid, M.S. Elshikh, One-pot biosynthesis of reduced graphene oxide/prussian blue microcubes composite and its sensitive detection of prophylactic drug dimetridazole, J. Electrochem. Soc. 165 (2018) B27–B33.

[19] O. Alévêque, P.-Y. Blanchard, C. Gautier, M. Dias, T. Breton, E. Levillain, Electroactive self-assembled monolayers: Laviron's interaction model extended to non-random distribution of redox centers, Electrochem. Commun. 12 (2010) 1462–1466.

[20] D. Chen, J. Deng, J. Liang, J. Xie, K. Huang, C. Hu, Core–shell magnetic nanoparticles with surface-imprinted polymer coating as a new adsorbent for solid phase extraction of metronidazole, Anal. Methods. 5 (2013) 722–728.

[21] S. Lú, K. Wu, X. Dang, S. Hu, Electrochemical reduction and voltammetric determination of metronidazole at a nanomaterial thin film coated glassy carbon electrode, Talanta 63 (2004) 653–657.

[22] P. Zuman, Z. Fijalek, Contribution to the understanding of the reduction mechanism of nitrobenzene, J. Electroanal. Chem. Interfacial Electrochem. 296 (1990) 583–588.

[23] Y. Gu, X. Yan, C. Li, B. Zheng, Y. Li, W. Liu, Z. Zhang, M. Yang, Biomimetic sensor based on molecularly imprinted polymer with nitroreductase-like activity for metronidazole detection, Biosens. Bioelectron. 77 (2016) 393–399.

[24] E. Daeseleire, H. De Ruyck, R. Van Renterghem, Rapid confirmatory assay for the simultaneous detection of ronidazole, metronidazole and dimetridazole in eggs using liquid chromatography-tandem mass spectrometry, Analyst 125 (2000) 1533–1535.

[25] M.J. Sams, P.R. Strutt, K.A. Barnes, A.P. Damant, M.D. Rose, Determination of dimetridazole, ronidazole and their common metabolite in poultry muscle and eggs by high performance liquid chromatography with UV detection and confirmatory analysis by atmospheric pressure chemical ionisation mass spectrometry†‡, Analyst 123 (1998) 2545–2549.

[26] S.-H. Chang, Y.-H. Lai, C.-N. Huang, G.-J. Peng, C.-D. Liao, Y.-M. Kao, S.-H. Tseng, D.-Y. Wang, Multi-residue analysis using liquid chromatography tandem mass spectrometry for detection of 20 coccidiostats in poultry, livestock, and aquatic tissues, J. Food Drug Anal. 27 (2019) 703–716.